

Efficient solvent free synthesis of tertiary α -aminophosphonates using $H_2Ti_3O_7$ nanotubes as a reusable solid-acid catalyst

Bhoomireddy Rajendra Prasad Reddy,^a Peddiahgari Vasu Govardhana Reddy*^a and Bijivemula. N. Reddy^b

^a Department of Chemistry, Yogi Vemana University, Kadapa-516003, Andhra Pradesh, India.

^b Department of Chemistry, Vellore Institute of Technology, Vellore-632014, Tamil Nadu, India.

Table of Contents

1. General experimental details	S2-S3
2. Catalyst characterization	S3-S6
2.1. HR-TEM image of (a) TFP, (b) TNP and (c & d) TNR	S3-S4
2.2. XRD Pattern of TFP, TNP and TNR	S4-S5
2.3. N ₂ Adsorption-desorption Isotherm of TNP, TNR and TNT	S5
2.4. BJH pore size distributions for TNP, TNR and TNT	S6
2.5. NH ₃ -TPD of TFP, TNP, TNR and TNT	S6
3. Characterization data of novel α-aminophosphonates	S7-S8
4. NMR (¹H, ¹³C & ³¹P) and Mass spectra of novel α-aminophosphonates	S9-S15
5. References	S15

1. General experimental details

Photo catalyst grade titanium dioxide (TiO₂-P25 and TiO₂-LAB) was procured from Degussa Corporation, Germany and Merck, India. Sodium Hydroxide pellets (99 %) and Hydrochloric acid (35 % pure) was purchased from Merck, India. Distilled water was used for materials synthesis/solution preparation. De-ionized water used for nanotube washing process.

Solvents were purchased from Merck, India and used as received. Analytical thin layer chromatography was performed with aluminium backed plates pre-coated with silica gel 60 F254 (0.2 mm) from Merck, and visualization was achieved by inspection under 254nm UV light. Column chromatography was performed using silica gel (100 - 200 mesh) from SDFCL; eluting solvents reported as % v/v mixtures.

Powder wide-angle X-ray diffraction (WAXRD) patterns of the catalysts were recorded using a D8 ADVANCE X-ray diffractometer (Bruker) equipped with Ni-filtered Cu K_α ($k = 1.5418 \text{ \AA}$) radiation (30 kV, 50 mA). Transmission electron microscopy (TEM) and high resolution transmission electron microscopy (HRTEM) measurements were carried out by using a FEI Tecnai F20ST electron microscope operated at 200 keV and equipped with high angle annular dark field (HAADF) detector and energy dispersive X-ray (EDX) spectrometer. For TEM measurement, all the catalysts were sonicated in acetone or ethanol and the resulting dispersion of the powder catalysts was transferred into a holey carbon film fixed on a 3 mm copper grid (200 meshes). The specific surface area (SSA) and pore size of the catalysts were measured by N₂ adsorption-desorption isotherms at 77 K using a surface area analyzer (Micromeritics, ASAP 2020). Prior to the measurements, all the catalysts were degassed at 350 °C under vacuum (10^{-3} mbar) for 6 h. Brunauer-Emmett-Teller method (BET) was used to calculate the SSA whereas the pore size distributions were derived from the desorption branches of the isotherms based on the Barrett-Joyner-Halenda model (BJH).

Total acidity was evaluated by temperature-programmed desorption of ammonia (TPD/NH₃) using a Micromeritics Chemisorb 2750 instrument. Before NH₃ desorption, the samples were heated to 200 °C ($20^\circ \text{ min}^{-1}$) in 30mL high pure Helium flow. Subsequently, the samples were cooled down to 30 °C in helium flow. NH₃ adsorption was performed under ambient conditions and saturated for about 30 min in a flow of 10% ammonia in Helium (30 ml min^{-1}). Then, the samples were purged in a Helium flow until a constant baseline level was

attained. Desorption of NH_3 was carried out with the linear heating rate ($10^\circ\text{C min}^{-1}$) in a flow of Helium from 30°C - 600°C .

Infrared spectra of the title compounds were recorded on Bruker Alpha-Eco ATR-FTIR (Attenuated total reflection-Fourier transform infrared) interferometer with single reflection sampling module equipped with ZnSe crystal. NMR analysis was performed on Bruker DRX 400 (400 MHz for ^1H NMR and 100 MHz for ^{13}C NMR) and Bruker DRX 500 (500 MHz for ^1H NMR and 100 MHz for ^{13}C NMR) spectrometers. Chemical shifts are expressed as δ (ppm) values using TMS or the residual signals of the solvents as the internal standard. Mass spectra were recorded on a Finnigan MAT 1020 mass spectrometer operating 70 eV. Melting points were recorded on Guna melting point apparatus and are uncorrected.

2. Catalyst characterization

2.1. HR-TEM image of (a) TFP, (b) TNP and (c & d) TNR

Fig. S1 Shows that the HR-TEM images of TiO_2 -fine particles (TP), TiO_2 -P25 nanoparticles (TNP), $\text{H}_2\text{Ti}_3\text{O}_7$ nanorods (TNR) catalysts. The **fig. S1a** represents those TiO_2 fine particles with ~ 150 nm and **fig. S1b** displays that TiO_2 nanoparticles with size ~ 25 nm with well dispersed manner. **Fig. S1c** depicts rod-like spherical morphology having different length > 1 μm . **Fig. S1d** confirms the clean nanorods surface with completely filled-inside, besides lattice arrangements observed.

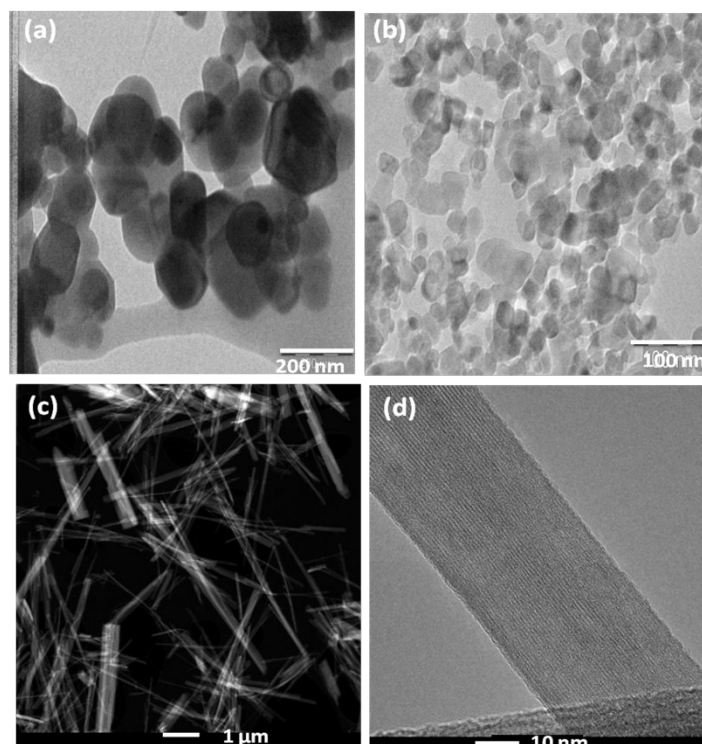


Fig. S1 HR-TEM image of (a) TP, (b) TNP and (c & d) TNR

2.2. XRD Pattern of TFP, TNP and TNR

Fig. S2 displays XRD pattern of standard TFP, TNP and TNR. TNP catalyst shows major peaks at $2\theta = 25.4$ and 27.5° are characteristic pattern of tetragonal structure of anatase and rutile phase respectively (JCPDS No.21-1272 & 21-1276). TFP catalyst show major peak at $2\theta = 25.4$ are characteristic pattern of tetragonal structure of anatase phase (JCPDS No.21-1272). The sharp peaks indicate the high crystallinity of the TiO_2 nanoparticles. The TNR catalyst shows 3 major diffraction peaks at $2\theta = 10.2$, 24.1 , and 48.2° is matches well with hydrogen trititanate phase ($\text{H}_2\text{Ti}_3\text{O}_7$), layered type and monoclinic crystal structure (JCPDS No. 47-0561 and 31-1329). The broad diffraction pattern of TNR suggests that the poor crystallinity of the catalytic materials. These observations are matches well with our earlier reports.^{1a, 1b}

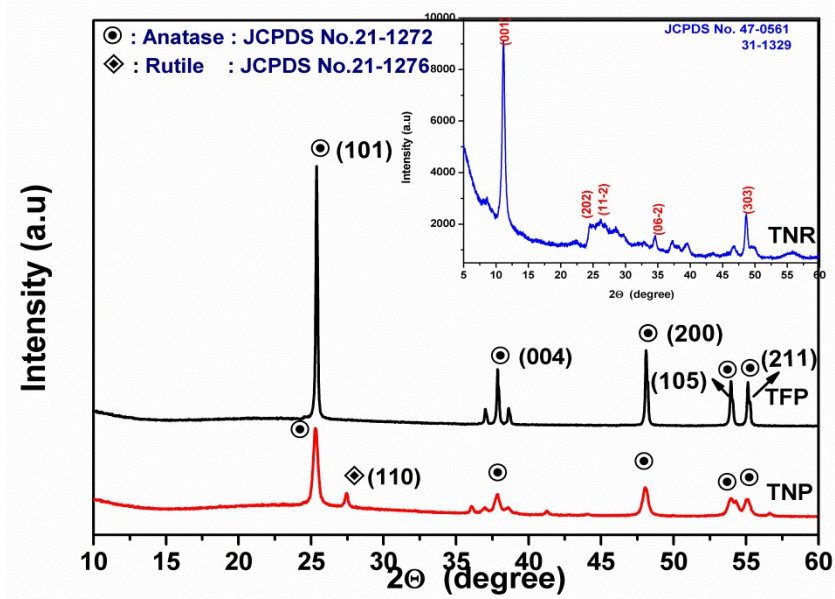


Fig. S2 XRD Pattern of TFP, TNP and TNR

2.3. N₂ Adsorption-desorption Isotherm of TNP, TNR and TN

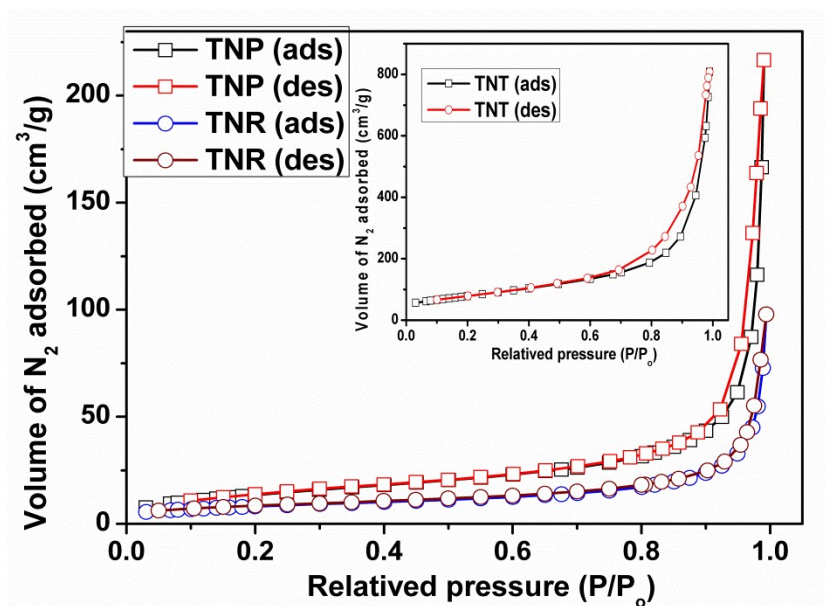


Fig. S3 N₂ Adsorption-desorption Isotherm of TNP, TNR and TNT

2.4. BJH pore size distributions for TNP, TNR and TNT

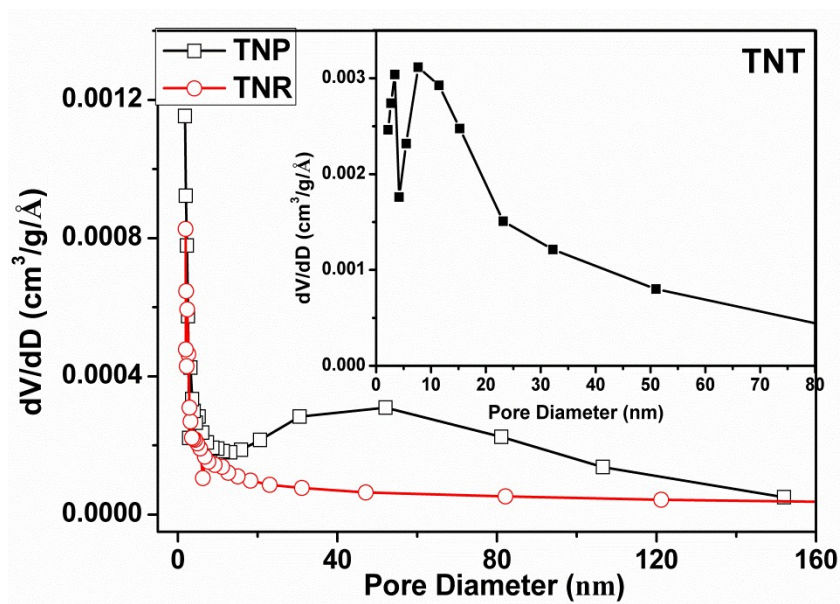


Fig. S4 BJH pore size distributions for TNP, TNR and TNT

2.5. NH_3 -TPD of TFP, TNP, TNR and TNT

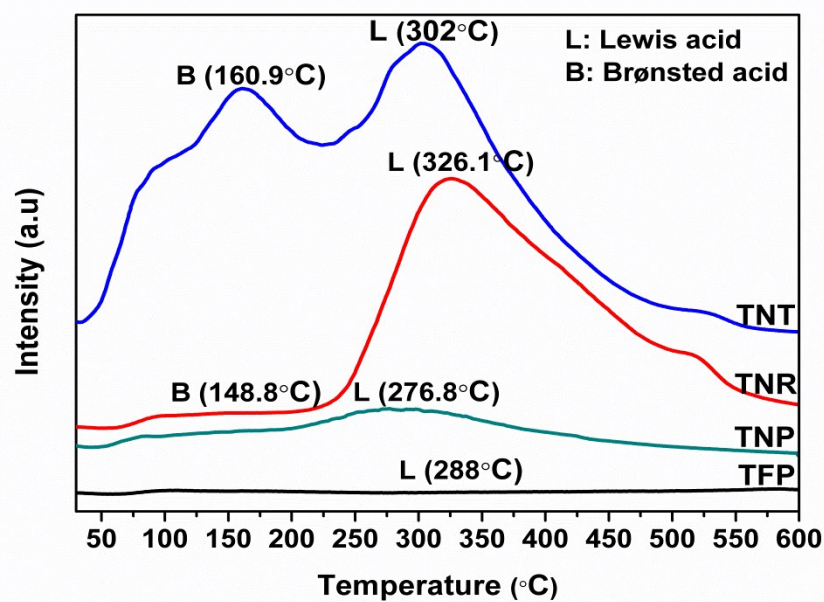


Fig. S5 NH_3 -TPD of TFP, TNP, TNR and TNT

3. Characterization data of novel α -aminophosphonates

Diethyl [5,8-dioxa-10-azadispiro[2.0.4.3]undec-10-yl(2-thienyl)methyl]phosphonate (17)

Brown colour oil; IR, ν_{\max} (ZnSe)/ cm^{-1} : 3081 (Ar-C-H), 2980 (ali-C-H), 1225 (P=O), 1222 (C-N), 960 (P-O), 795 (P-C); ^1H NMR (400 MHz, CDCl_3 , δ ppm): 7.29 (d, $J = 6.4$ Hz, 1H, Ar-H), 7.17 (s, 1H, Ar-H), 7.02 (t, $J = 12.4$ Hz, Ar-H), 4.29-4.15 (m, 3H, -P(O)CH- & -P(O)OCH₂CH₃), 4.07-3.89 (m, 2H, -P(O)OCH₂CH₃), 3.87-3.72 (m, 4H, -OCH₂CH₂O-), 3.11 (d, $J = 10$ Hz, 1H, -N-CH₂), 2.93 (d, $J = 7.6$ Hz, -N-CH₂), 2.03 (d, $J = 9.6$ Hz, -N-CH₂), 1.39-1.25 (m, 3H, -P(O)OCH₂CH₃), 1.17-1.14 (m, 3H, -P(O)OCH₂CH₃), 0.83-0.81 (m, 2H, cyclopropyl-CH₂), 0.53-0.46 (m, 2H, cyclopropyl-CH₂); ^{13}C NMR (100 MHz, CDCl_3 , δ ppm): 133.85 (Ar-C), 128.80 (Ar-C), 126.70 (Ar-C), 125.88 (Ar-C), 113.42 (CH₂O-C-OCH₂), 64.50 (-P(O)OCH₂CH₃), 63.39 (-OCH₂CH₂O-), 62.82 (-N-CH₂), 61.12 (-N-CH₂), 60.51 (qr, $J = 144.5$, -P(O)-CH-N-), 16.50 (-P(O)OCH₂CH₃), 9.31 (cyclopropyl-CH₂); ^{31}P NMR (161 MHz, CDCl_3 , δ ppm): 19.89 (s); MS (ESI): 388.1348 ([M+H]⁺). Anal. Calcd for C₁₇H₂₇NO₅PS: C, 52.70; H, 6.76; N, 3.62%; Found: C, 52.75; H, 5.70; N, 3.68%.

Dibutyl [5,8-dioxa-10-azadispiro[2.0.4.3]undec-10-yl(2-thienyl)methyl]phosphonate (18)

Brown colour oil; IR, ν_{\max} (ZnSe)/ cm^{-1} : 3082 (Ar-C-H), 2959 (ali-C-H), 1230 (P=O), 1218 (C-N), 981 (P-O), 781 (P-C); ^1H NMR (500 MHz, CDCl_3 , δ ppm): 7.28 (m, 1H, Ar-H), 7.15 (s, 1H, Ar-H), 7.00-6.98 (qr, $J = 4.0$ Hz, 1H, Ar-H), 4.27 (d, 1H, $J = 21.0$ Hz, -P(O)CH-), 4.18-3.73 (m, 8H, -P(O)OCH₂CH₂CH₂CH₃ & -OCH₂CH₂O-), 3.09 (d, 1H, -N-CH₂), 2.91-2.88 (qr, $J = 6.5$ Hz, 2H, -N-CH₂), 2.80 (d, $J = 9.0$ Hz, 1H, -N-CH₂), 1.65-1.62 (m, 2H, -P(O)OCH₂CH₂CH₂CH₃), 1.48-1.45 (m, 2H, -P(O)OCH₂CH₂CH₂CH₃), 1.39-1.35 (m, 2H, -P(O)OCH₂CH₂CH₂CH₃), 1.26-1.21 (m, 2H, -P(O)OCH₂CH₂CH₂CH₃), 0.92 (t, $J = 9$ Hz, 3H, -P(O)OCH₂CH₂CH₂CH₃), 0.83-0.79 (m, 5H, -P(O)OCH₂CH₂CH₂CH₃ & cyclopropyl-CH₂), 0.48-0.47 (m, 2H, cyclopropyl-CH₂); ^{13}C NMR (100 MHz, CDCl_3 , δ ppm): 134.00 (Ar-C), 128.76 (Ar-C), 126.69 (Ar-C), 125.82 (Ar-C), 113.45 (CH₂O-C-OCH₂), 67.05 (-P(O)OCH₂CH₂-CH₂CH₃), 66.40 (-OCH₂CH₂O-), 64.52 (-N-CH₂), 61.11 (-N-CH₂), 60.31 (qr, $J = 153.75$, -P(O)-CH-N-), 32.62 (-P(O)OCH₂CH₂CH₂CH₃), 18.70 (-P(O)OCH₂CH₂CH₂CH₃), 13.59 (-P(O)OCH₂CH₂-CH₂CH₃), 9.32 (cyclopropyl-CH₂); ^{31}P NMR (202 MHz, CDCl_3 , δ ppm): 19.90-19.80 (qr); HRMS: Anal. Calcd for C₂₄H₁₉N₂O₄PS (M+H): 444.19681; found: 444.19620.

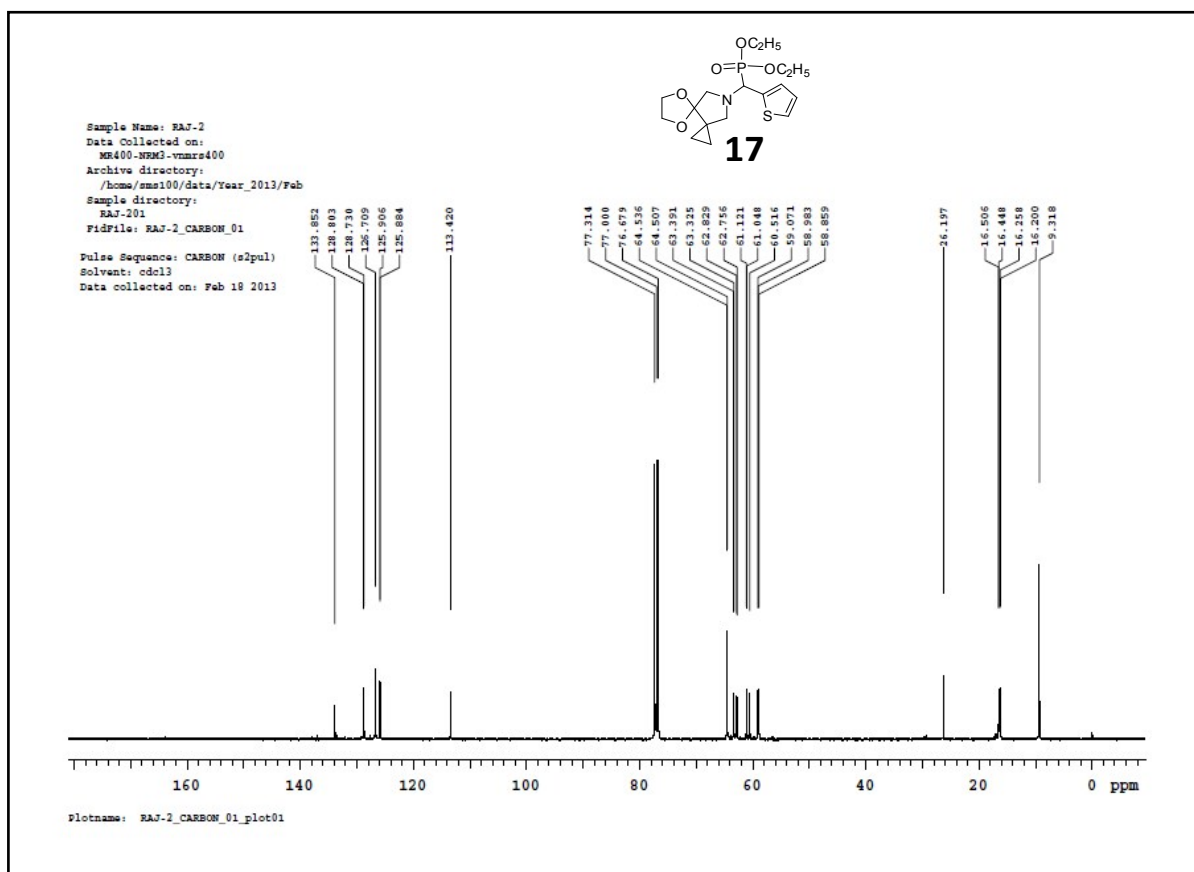
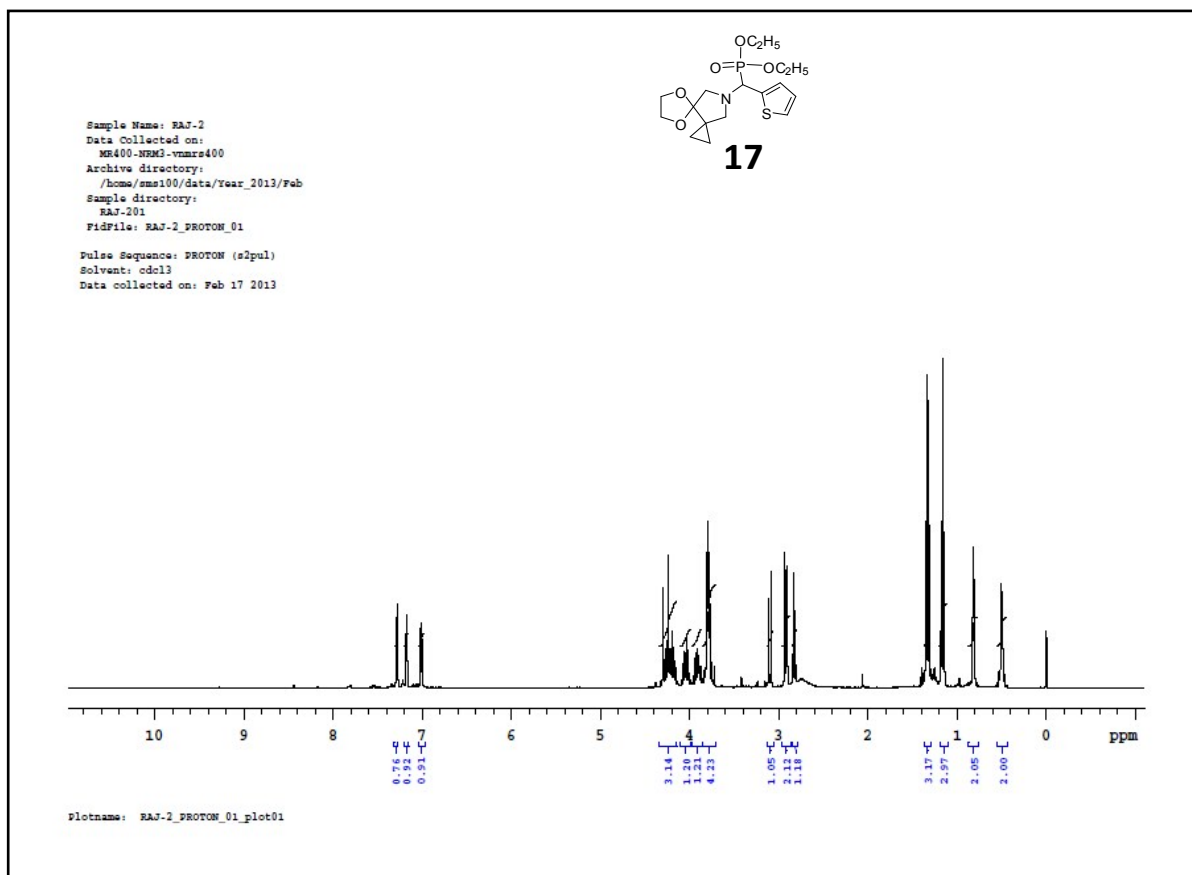
Dibutyl[(2,6-dimethoxy-3-pyridyl)(5,8-dioxa-10-azadispiro[2.0.4.3]undec-10-yl)methyl]phosphonate (19)

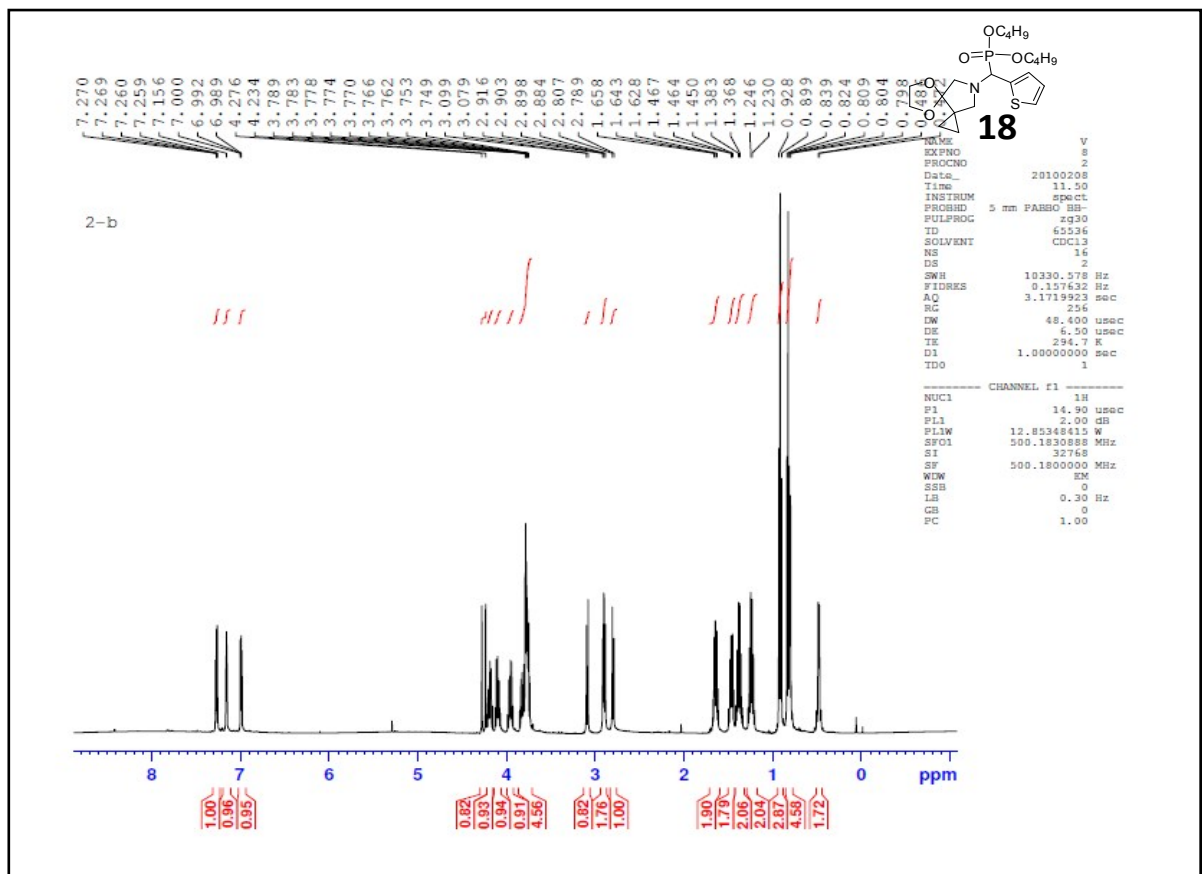
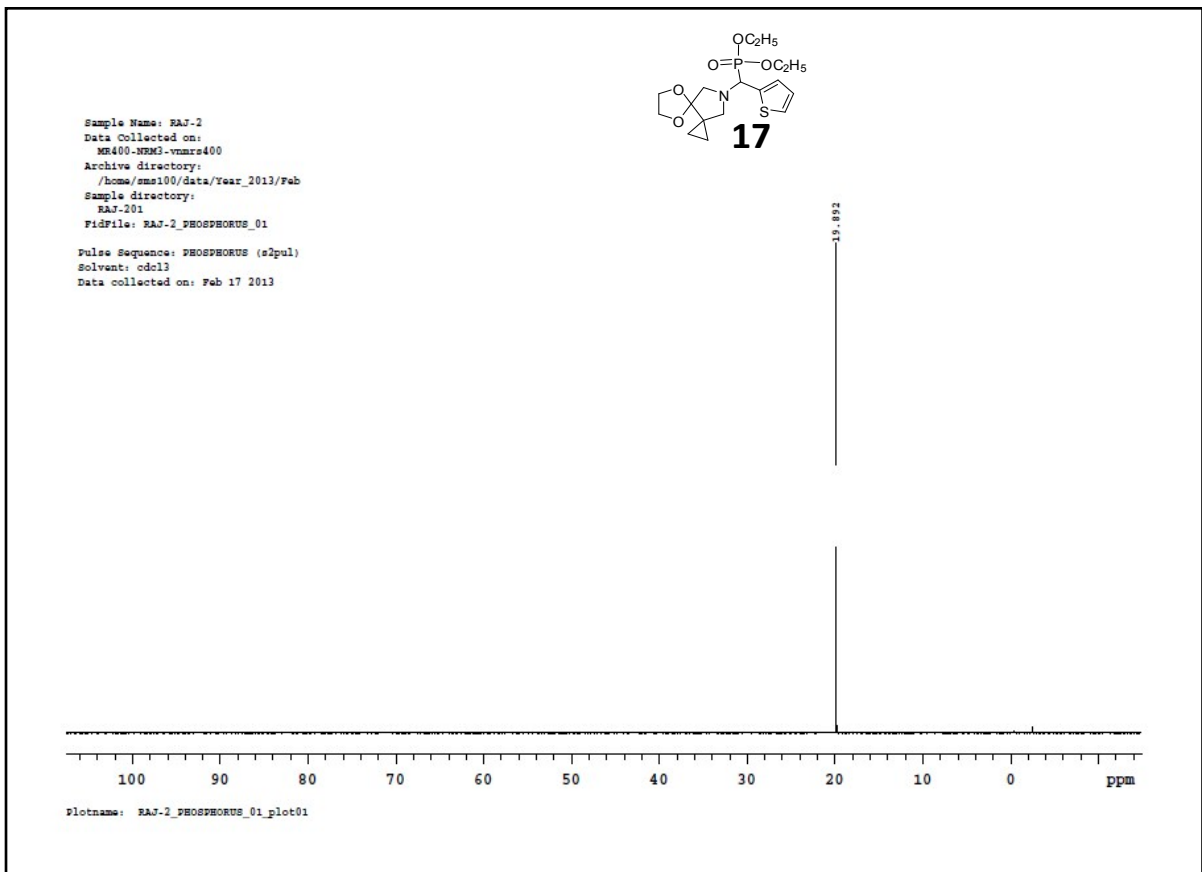
Brown colour oil; IR, ν_{max} (ZnSe)/ cm^{-1} : 3026 (Ar-C-H), 2892 (ali-C-H), 1548 (C=N), 1265 (P=O), 1175 (C-O), 1087 (C-N), 967 (P-O), 788 (P-C); ^1H NMR (400 MHz, CDCl_3 , δ ppm): 7.96 (d, $J = 10.0$ Hz, 1H, Ar-H), 6.36 (d, $J = 7.6$ Hz, 1H, Ar-H), 4.57 (d, $J = 18.8$ Hz, 1H, -P(O)CH-), 4.15-3.75 (m, 14H, -P(O)OCH₂CH₂CH₂CH₃ & -OCH₂CH₂O- & Ar-OCH₃), 3.33 (s, 2H, -N-CH₂), 3.15 (d, $J = 9.2$ Hz, 1H, -N-CH₂), 3.08 (d, $J = 9.2$ Hz, -N-CH₂), 1.67-1.60 (m, 2H, -P(O)OCH₂CH₂CH₂CH₃), 1.45-1.34 (m, 6H, -P(O)OCH₂CH₂CH₂CH₃ & -P(O)OCH₂CH₂CH₂CH₃), 1.25-1.20 (m, 6H, -P(O)OCH₂CH₂CH₂CH₃), 0.85-0.83 (t, $J = 16.0$ Hz, 4H, cyclopropyl-CH₂); ^{13}C NMR (100 MHz, CDCl_3 , δ ppm): 162.76 (Ar-C), 160.88 (Ar-C), 142.52 (Ar-C), 105.88 (CH₂O-C-OCH₂), 101.03 (Ar-C), 66.48 (-P(O)OCH₂CH₂CH₂CH₃), 60.73 (Ar-OCH₃), 57.04 (-OCH₂CH₂O-), 55.37 (-P(O)-CH-N-), 53.52 (-N-CH₂), 32.56 (-P(O)OCH₂CH₂CH₂CH₃), 18.69 (-P(O)OCH₂CH₂CH₂CH₃), 16.57 (-P(O)OCH₂CH₂CH₂CH₃), 13.57 (cyclopropyl -CH₂); ^{31}P NMR (162 MHz, CDCl_3 , δ ppm): 22.05 (s); MS (ESI): 499.1573 ([M+H]⁺). Anal. Calcd for C₂₄H₄₀N₂O₇P: C, 57.70; H, 8.07; N, 5.61%; Found: C, 57.75; H, 8.09; N, 5.75%.

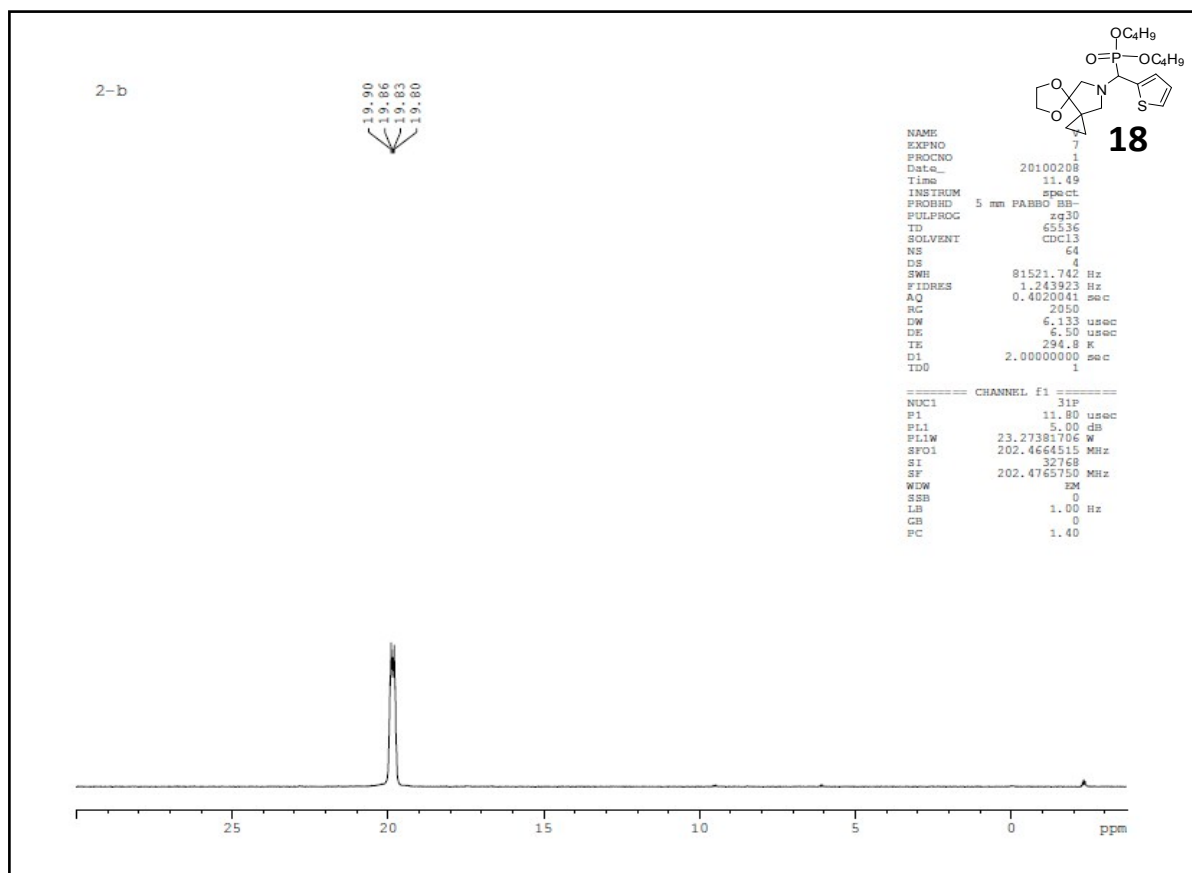
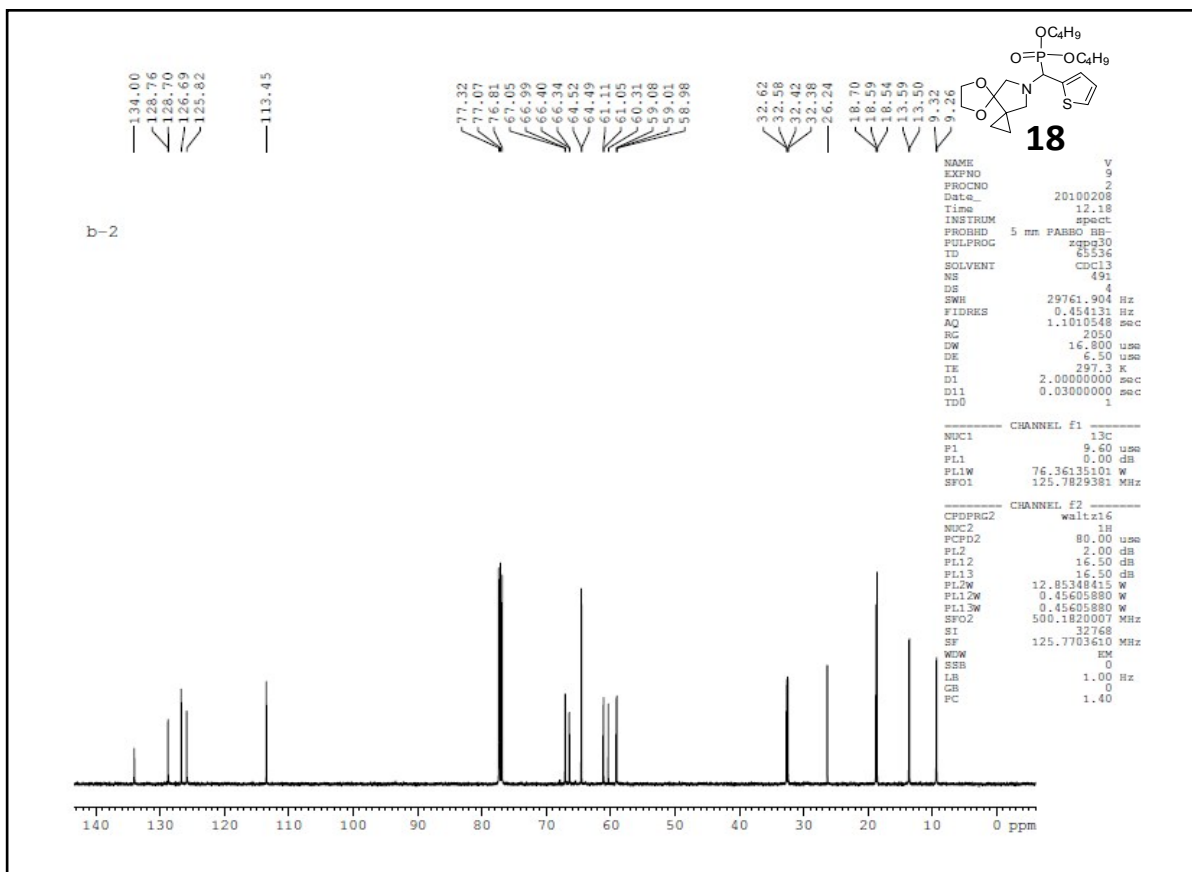
Diethyl[5,8-dioxa-10-azadispiro[2.0.4.3]undec-10-yl[3-(5-pyrimidinyl)phenyl]methyl]phosphonate (20)

Brown colour oil; IR, ν_{max} (ZnSe)/ cm^{-1} : 3087 (Ar-C-H), 2935 (ali-C-H), 1620 (C=N), 1236 (P=O), 1175 (C-O), 1027 (C-N), 965 (P-O), 788 (P-C); ^1H NMR (400 MHz, CDCl_3 , δ ppm): 9.22 (s, 1H, Ar-H), 8.96 (s, 2H, Ar-H), 7.73-7.69 (m, 1H, Ar-H), 7.58-7.55 (m, 1H, Ar-H), 7.53-7.26 (m, 2H, Ar-H), 4.29-4.15 (m, 3H, -(P)CH- & -P(O)OCH₂CH₃), 4.07-3.89 (m, 2H, -P(O)OCH₂CH₃), 3.87-3.72 (m, 4H, -OCH₂CH₂O-), 3.11 (d, $J = 10.0$ Hz, 1H, -N-CH₂), 2.93 (d, $J = 7.6$ Hz, -N-CH₂), 2.03 (d, $J = 9.6$ Hz, -N-CH₂), 1.39-1.25 (m, 3H, -P(O)OCH₂CH₃), 1.17-1.14 (m, 3H, -P(O)OCH₂CH₃), 0.83-0.81 (m, 2H, cyclopropyl-CH₂), 0.53-0.46 (m, 2H, cyclopropyl-CH₂); ^{13}C NMR (100 MHz, CDCl_3 , δ ppm): 157.53 (Ar-C), 154.94 (Ar-C), 136.13 (Ar-C), 134.21 (Ar-C), 130.70 (Ar-C), 129.31 (Ar-C), 128.43 (Ar-C), 126.57 (Ar-C), 113.40 (CH₂O-C-OCH₂), 66.49 (-P(O)OCH₂CH₃), 64.60 (-OCH₂CH₂O-), 63.04 (-N-CH₂), 60.85 (-P(O)-CH-N-), 32.53 (-P(O)OCH₂CH₃), 9.58 (cyclopropyl-CH₂); ^{31}P NMR (162 MHz, CDCl_3 , δ ppm): 20.83 (t, $J = 13.4$ Hz); MS (ESI): 460.2001 ([M+H]⁺). Anal. Calcd for C₂₃H₃₁N₃O₅P: C, 59.99; H, 6.79; N, 9.13%; Found: C, 60.05; H, 6.84; N, 9.18%.

4. ¹H, ¹³C and Mass spectra of novel α-aminophosphonates

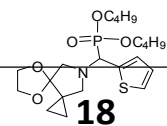




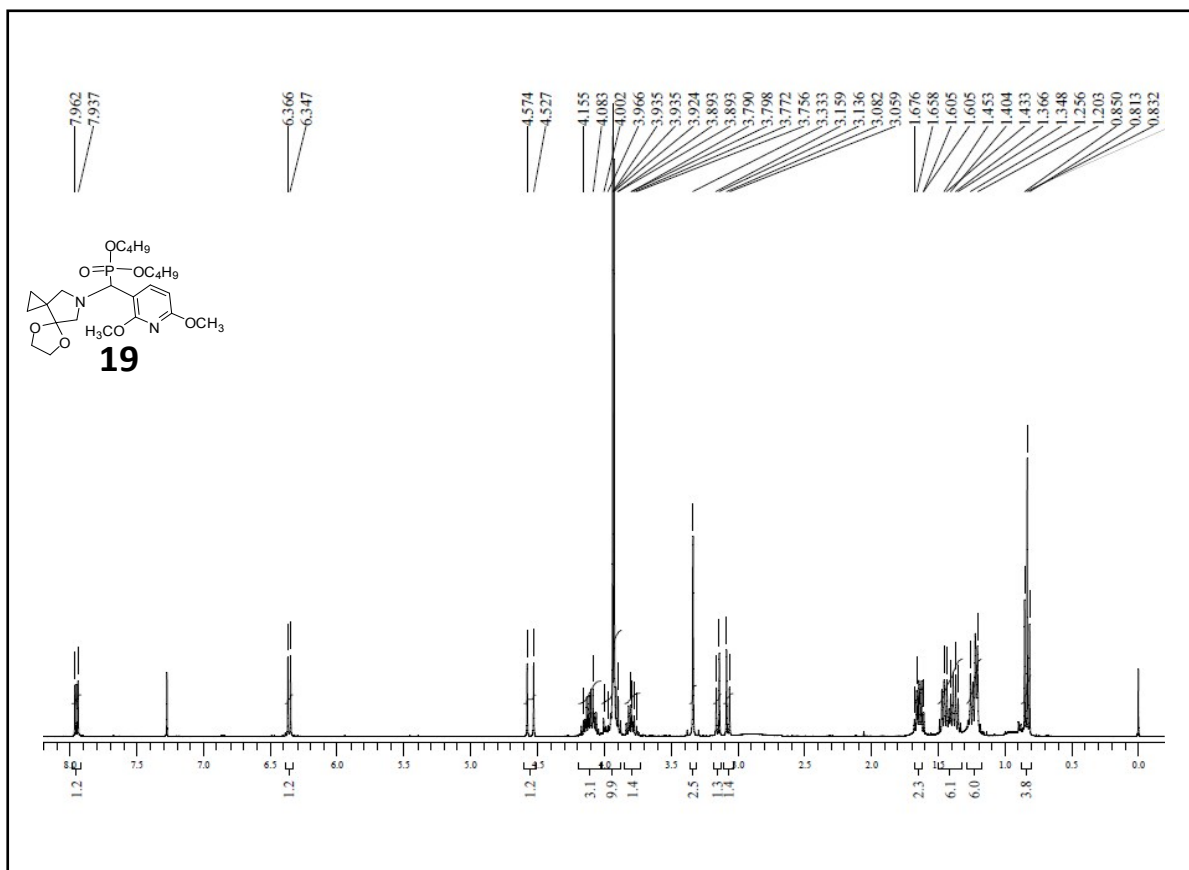
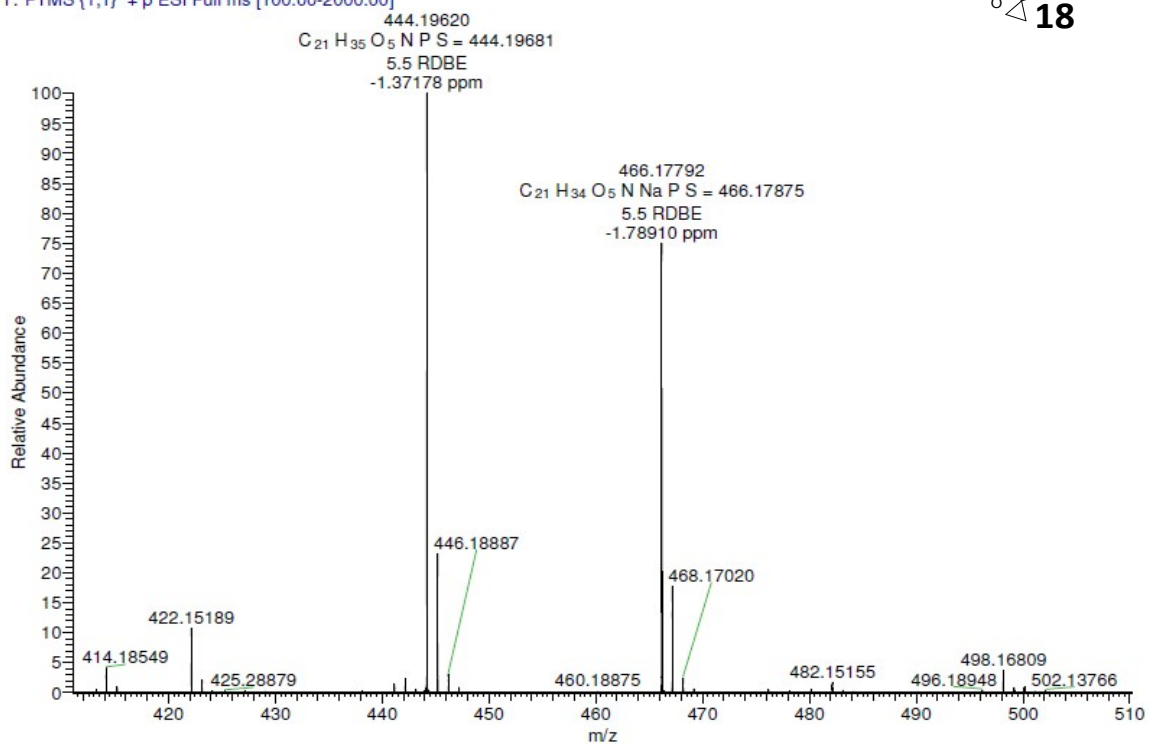


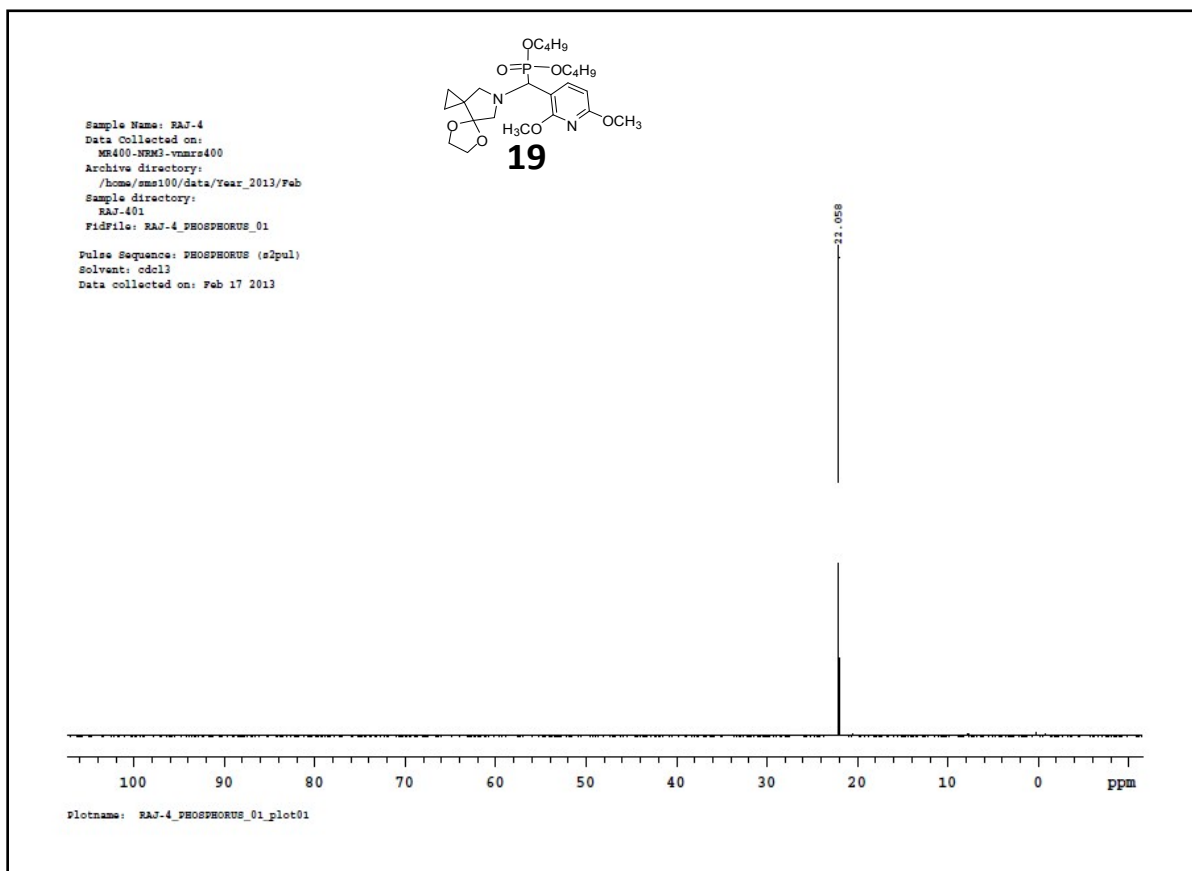
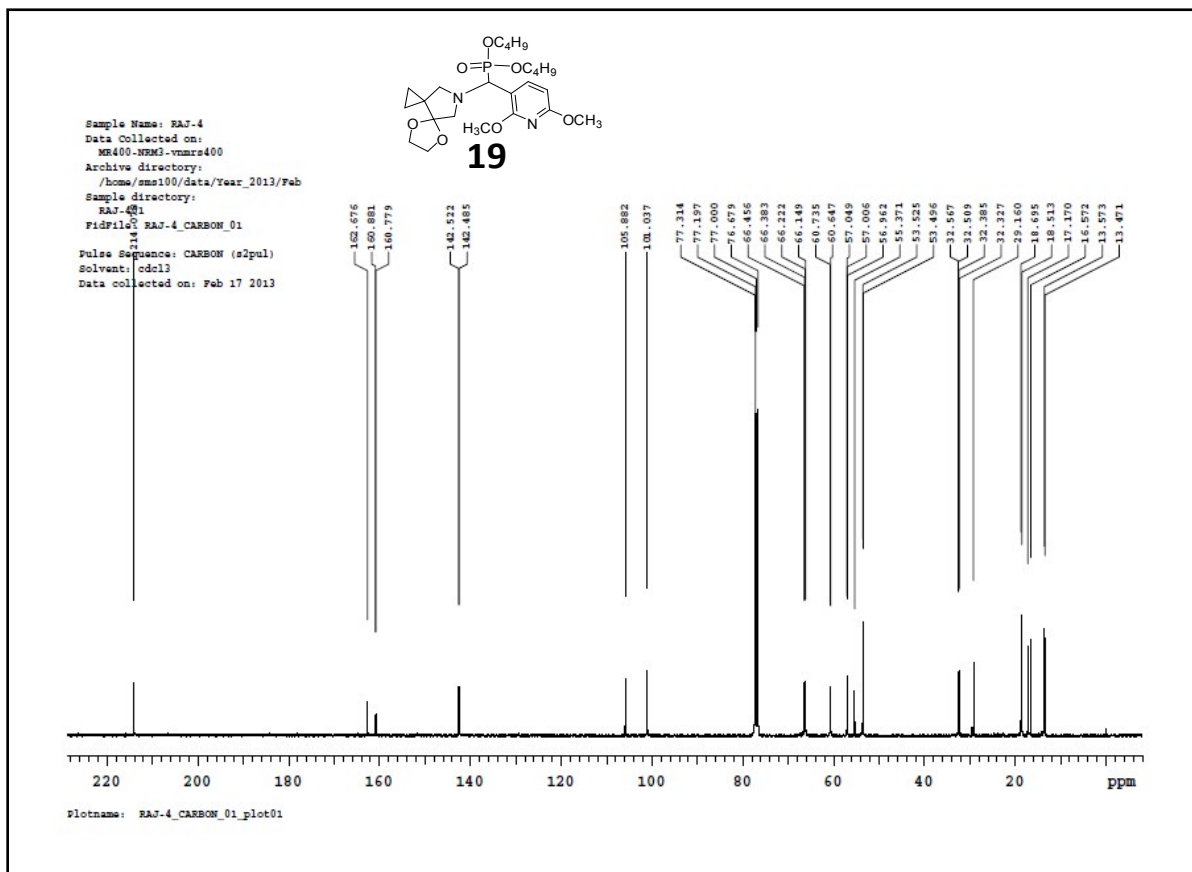
P.J. REDDY
1/8/2013 4:53:17 PM

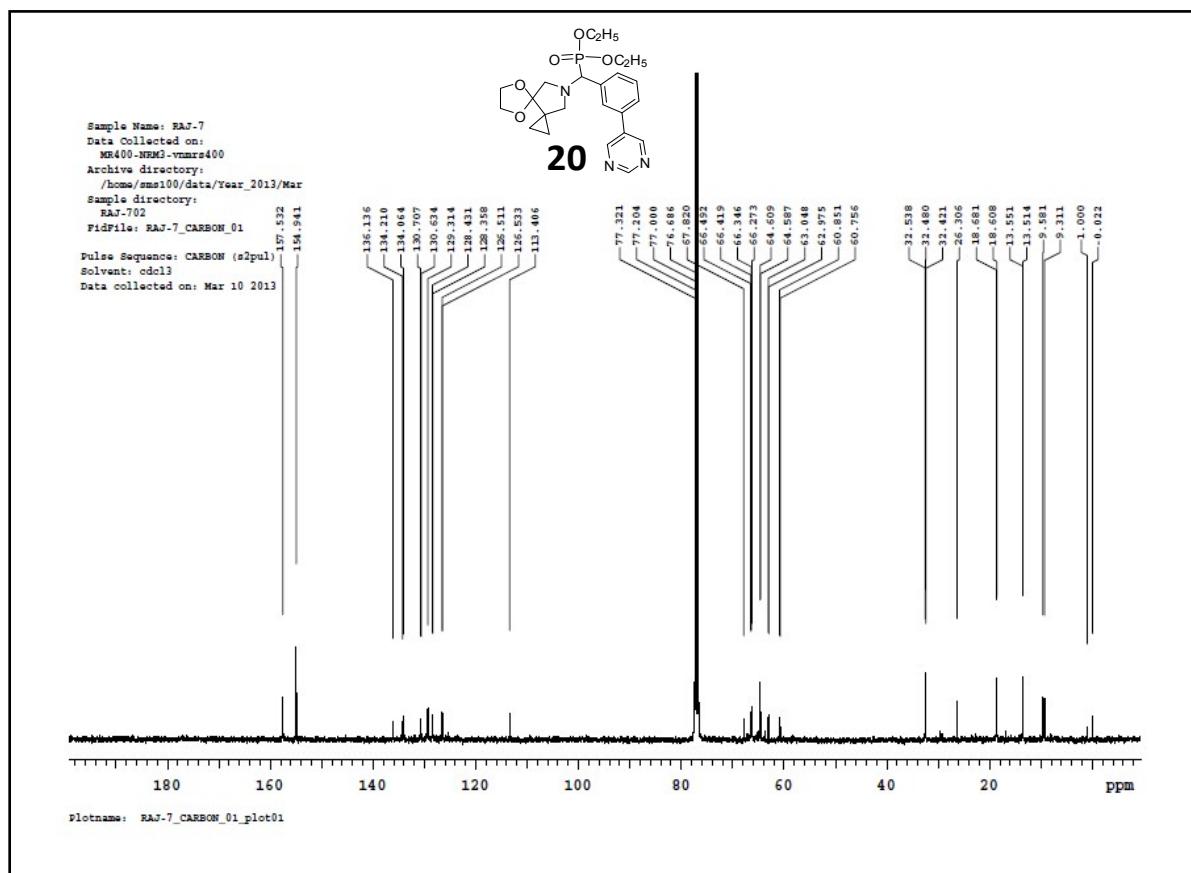
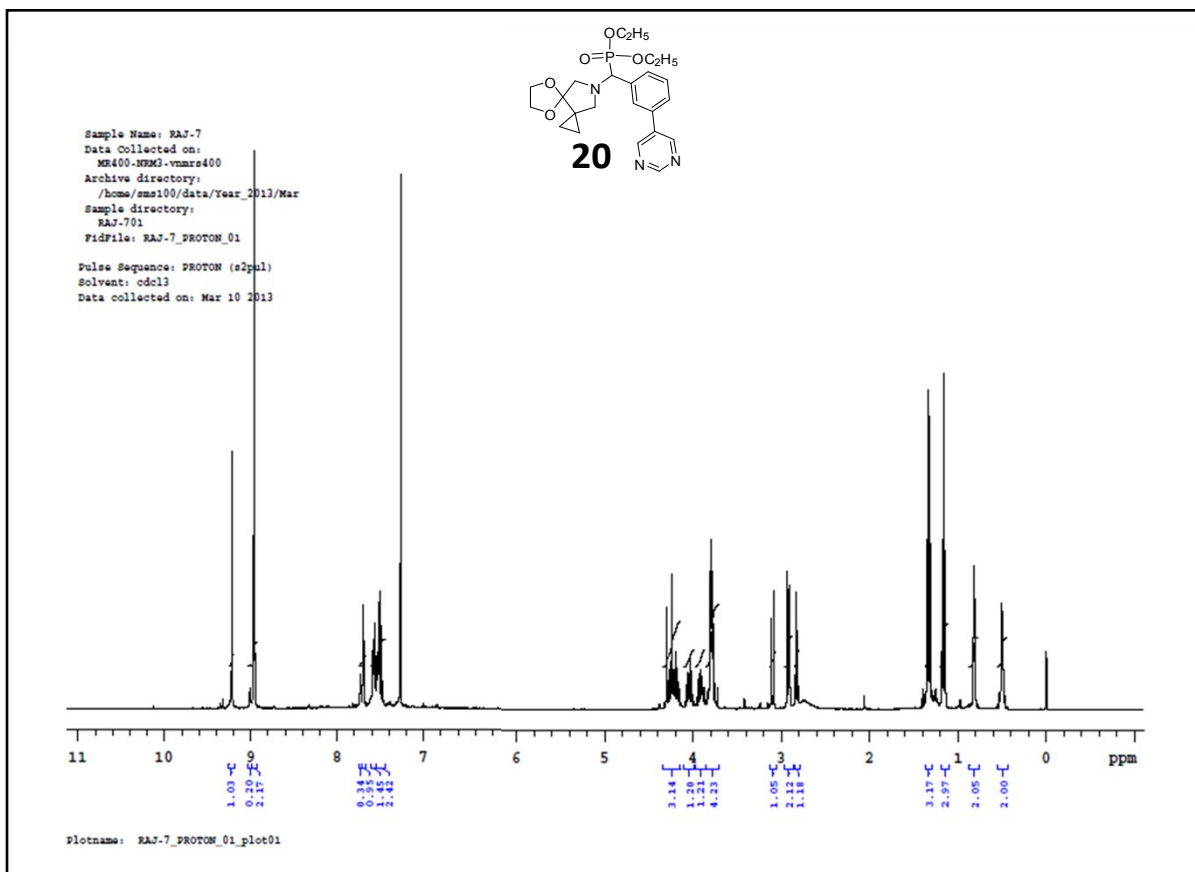
INDIAN INSTITUTE OF CHEMICAL TECHNOLOGY
NATIONAL CENTRE FOR MASS SPECTROMETRY

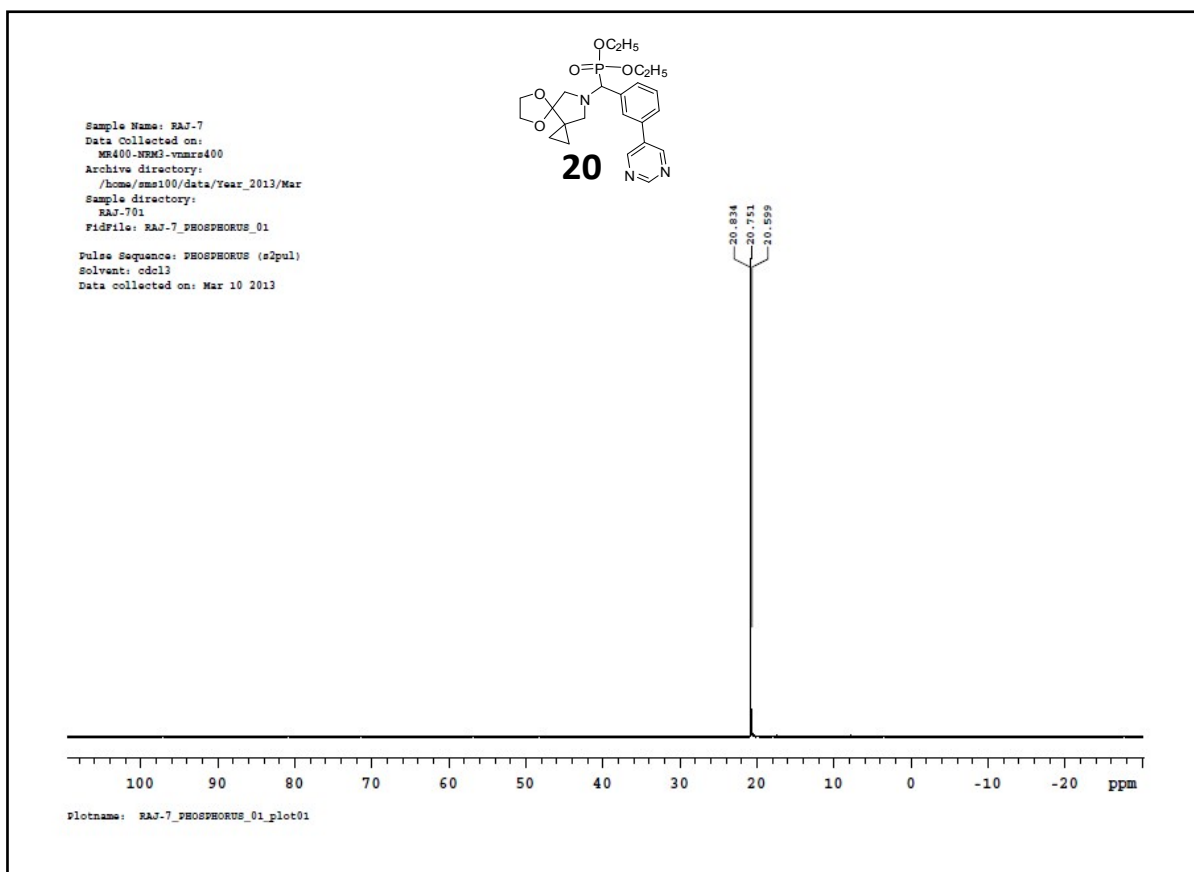


JSY-SY-2 #39 RT: 0.40 AV: 1 NL: 1.74E7
T: FTMS (1,1) + p ESI Full ms [100.00-2000.00]









5. References

- (a) Shankar, M. V.; Anandan, S.; Venkatachalam, N.; Arabindoo, B.; Murugesan, V.; *Chemosphere*, **2006**, *63*, 1014-1021; (b) Praveen Kumar, D.; Lakshmana Reddy, N.; Mamatha Kumari, M.; Srinivas, B.; Durga kumari, V.; Sreedhar, B.; Roddatis, V.; Bondarchuk, O.; Karthik, M.; Neppolian, B.; Shankar, M. V. *Sol. Energy Mater. Sol. Cells*, **2015**, *136*, 154-166.